RSC Advances

PAPER

View Article Online
View Journal | View Issue

Cite this: *RSC Adv.*, 2023, **13**, 6760

One-pot hydrothermal synthesis of metal-doped carbon dot nanozymes using protein cages as precursors

Yanfang Shen, [a] Ruofei Zhang[b] and Ying Wang *[a]

Received 14th November 2022
Accepted 10th January 2023

DOI: 10.1039/d2ra07222j

rsc.li/rsc-advances

Metal-doped carbon dots represent a new class of promising nanomaterials with enzyme-like activity, whose properties such as fluorescence properties and enzyme-like activity are determined by the precursors and the conditions used to prepare them. Nowadays, the synthesis of carbon dots using naturally occurring precursors has attracted increasing attention. Here, using metal-loaded horse spleen ferritin as a precursor, we report a facile one-pot hydrothermal strategy to synthesise metal-doped fluorescent carbon dots with enzyme-like activity. The as-prepared metal-doped carbon dots exhibit high water solubility, uniform size distribution, and good fluorescence. In particular, the Fe-doped carbon dots exhibit prominent oxidoreductase catalytic activities, including peroxidase-like, oxidase-like, catalase-like, and superoxide dismutase-like activities. This study provides a green synthetic strategy for developing metal-doped carbon dots with enzymatic catalytic activity.

Introduction

Nanozymes are a class of nanomaterials with enzyme-like activity. Compared with natural enzymes, nanozymes possess the advantages of high stability, adjustable activity, diversified functions, rational design and large-scale preparation. Since Yan's group reported the first peroxidase-like Fe_3O_4 nanozyme in 2007, thousands of nanozymes have been reported so far.[1–4] The types of nanozymes mainly include metal oxides, metal and carbon-based materials, *etc.*, with enzyme-like activities mainly including peroxidase, oxidase, catalase and superoxide dismutase (SOD) activities.[5–7] The excellent catalytic properties make nanozymes a promising class of useful alternatives in applications such as biochemical detection, medical diagnosis, and therapy.[8–10] However, biomedical applications of nanozymes have been hindered by biosafety issues, such as unknown biocompatibility and biodegradability, and potential toxicity risks.[11] In particular, metal-based or metal oxide nanomaterials may cause some health problems during translational medicine.[12] Therefore, there is an urgent need to develop nanozymes with biocompatible materials to meet the requirements for green and biosafe catalysts in the biomedical field.

Carbon dots (CDs) are an emerging zero-dimensional fluorescent nanomaterial with a size of less than 10 nm. In recent years, growing attention is focused on the development of CDs with enzyme-like activities, which has become a promising class of nanozymes.[13,14] CDs-based nanozymes possess the characteristics of low cost, simple preparation, high stability, and excellent fluorescence properties, and have better biocompatibility than metal or metal oxide nanozymes, so they have great application potential in photocatalysis, disease diagnosis, bioimaging and sensing.[15–18] CDs are generally synthesized by decomposition of large carbon particles (top-down approach) or by polymerization, dehydration, and carbonization of small organic molecules (bottom-up approach).[19] Synthetic precursors and conditions are the key factors affecting the enzymatic properties of CDs nanozymes. For instance, the peroxidase-like activity of CDs synthesized from L-glutamic acid was much higher than those obtained from glycine, L-glutamine and acetate.[20] Also, CDs prepared from different coal sources (anthracite and bituminous) have been reported to have significantly different SOD-like activities.[21] However, the enzymatic activities of unmodified or undoped CDs is generally low and difficult to apply directly.

Incorporation of heteroatoms into the nanostructures of CDs may lead to dramatic changes in their chemical compositions, electronic structures and nanostructures.[22] Compared with nonmetal atoms, metal atoms have more electrons and unoccupied orbitals and larger atomic radius, resulting in more drastic changes in the electron density distribution and energy gap of doped CDs, which may significantly affect the enzymatic performance of CDs.[23] The incorporation of transition metals such as Fe, Cu, or Mn into CDs has been reported to create highly active nanozymes with peroxidase-like and oxidase-like activities.[24–27] Most of the existing synthetic routes for metal-doped CDs use randomly combined organic molecules and

[a]*Department of Nuclear Medicine, The Fifth Affiliated Hospital, Sun Yat-sen University, Zhuhai City, Guangdong Province 519000, China. E-mail: wangy9@mail.sysu.edu.cn*
[b]*CAS Engineering Laboratory for Nanozyme, Key Laboratory of Protein and Peptide Pharmaceutical, Institute of Biophysics, Chinese Academy of Sciences, Beijing 100101, China*

metal ions as precursors, resulting in low yields. The lack of in-depth understanding of organic–metal interactions also leads to almost irreproducible synthesis of metal-doped CDs and difficulty in precise doping.[28] Therefore, there is an urgent need to find new synthetic methods to prepare metal-doped CDs.

Recently, high-yield non-metal-doped CDs have been synthesized simply, cheaply, scalable and rapidly from natural or bioderived precursors.[28–30] However, the synthesis of metal-doped CDs from biologically derived precursors has rarely been reported. Ferritin is a class of cage-like proteins consisting of 24 subunits with an outer diameter of 12 nm and a cavity with a diameter of 8 nm. Ferritin has a natural function of storing iron and can hold up to 4500 iron atoms. In recent years, ferritin has been found to be a versatile biomineralization reactor for loading various metals including Fe, Cu, Mn, Co, *etc*.[31] Importantly, metal-loaded ferritins have a well-defined protein shell-metal core spatial distribution.[32] Therefore, using ferritin as the precursor for the synthesis of CDs may be able to precisely dope metal atoms into the interior of CDs, which is difficult to achieve with existing synthetic strategies. Moreover, ferritin can be easily produced on a large scale by genetic engineering due to its high thermal stability. Therefore, metal-loaded ferritin may provide a green and ideal synthetic template for the precise synthesis of metal-doped CDs.

Here, using metal-loaded horse spleen ferritin as a precursor, we developed a facile one-pot hydrothermal method for the synthesis of metal-doped CDs nanozymes. During one-pot hydrothermal carbonization, metal ions enter the cavity of ferritin through ion transport channels, and then nucleate together with the protein cage. The synthesized metal-doped CDs exhibited good water solubility, uniform size and good fluorescence properties. Moreover, the incorporation of metals boosts the enzyme-like activity of CDs. In particular, Fe-doped CDs exhibit excellent oxidoreductase-like activity. This study demonstrates the feasibility of synthesizing metal-doped CDs using ferritin as a precursor, which provides a new strategy for the development of green high-performance CDs.

Materials and methods

Materials

Horse spleen apoferritin, quinine sulfate, hydrogen peroxide (H_2O_2, 30 wt%), and 3,3′,5,5′-tetramethylbenzidine (TMB) were purchased form Sigma Aldrich (Shanghai, China). Superoxide anion assay kit was purchased from DOJINDO (China).

Synthesis of M@Fn-CDs

To synthesize M@Fn-CDs, 100 mg horse spleen apoferritin was incubated with metal ions (including Co^{2+}, Fe^{2+}, Cu^{2+}, Mg^{2+}, Mn^{2+}, Ni^{2+}, Zn^{2+}, Gd^{2+}) at a molar ratio of 1 : 500 in 15 mL of 50 mM Tris–HCl buffer (pH 8.0) for 30 min. Subsequently, the ferritin solution loaded with metal ions was added to the hydrothermal reactor and heated at 200 °C for 12 h. The carbonized solution was filtered with a 0.22-micron filter, and then placed in a dialysis bag for dialysis against water for 24 h. The dialyzed solution was freeze-dried to finally obtain M@Fn-CDs powders. Metal-free Fn-CDs were also synthesized by the same method except that no metal ions were added.

Characterization

The morphological analysis of M@Fn-CDs in aqueous solution was performed on a Tecnai G2 F30 S-TWIN transmission electron microscope (TEM) with an operating voltage of 300 kV. The sizes of the M@Fn-CDs were obtained by measuring the particles in TEM images using ImageJ software. For each type of CDs, at least 100 particles from several TEM images were counted. The metal content in M@Fn-CDs was measured by using an inductively coupled plasma optical emission spectrometer (ICP-OES). The FT-IR spectra were acquired in the 4000–400 cm^{-1} range with a nominal resolution of 4 cm^{-1} on a Nicolet iS10 FT-IR spectrometer. UV/vis absorption spectra were recorded on a HITACHI U-3900 spectrophotometer using a pair of quartz cuvettes with a path length of 1 cm. The fluorescence properties of the samples were measured with a Hitachi F7000 spectrofluorophotometer.

Quantum yield

The absorbance at 350 nm and the peak area of the photoluminescence spectrum after excitation at 350 nm were measured for the quinine sulfate reference and M@Fn-CDs samples. Taking the absorbance as the abscissa and the fluorescence intensity (peak area) as the ordinate, the slope k was calculated. Then, the quantum yield was calculated by the following formula.

$$QY_{samp} = QY_{ref}\,(k_{samp}/k_{ref})(\eta_{samp}{}^2/\eta_{ref}{}^2)$$

where QY_{samp} is the quantum yield of the M@Fn-CDs sample, QY_{ref} is the quantum yield of quinine sulfate (55%), k_{samp} and k_{ref} are the slopes of the curves, and η_{samp} and η_{ref} are the refractive indices of the sample and reference, respectively.

Peroxidase-like activity assay

To measure peroxidase-like activity, 0.3 mg of M@Fn-CDs was first added to a cuvette containing 2 mL of NaAc-HAc buffer (0.2 M, pH 3.6). Subsequently, 100 μL of TMB solution (dissolved in DMSO, 10 mg mL^{-1}) was added to the cuvette, and the reaction mixture was incubated for 1 min in a dark thermostatic water bath at 37 °C. The peroxidase-catalyzed reaction was initiated by adding 900 μL of H_2O_2 (1 M, final concentration) to the reaction mixture, and the absorbance at 652 nm was measured 2 min later.

Oxidase-like activity assay

To measure oxidase-like activity, 0.6 mg of M@Fn-CDs was first added to a cuvette containing 3 mL of NaAc-HAc buffer (0.2 M, pH 3.6). Subsequently, 150 μL of TMB solution (dissolved in DMSO, 10 mg mL^{-1}) was added to the cuvette, and the absorbance at 652 nm was measured 2 min later.

Catalase-like activity assay

For the determination of catalase-like activity, 0.4 mg M@Fn-CDs was mixed with 5 mL of H_2O_2 aqueous solution (100 mM) under gentle stirring, and a specific oxygen electrode was used on a multiparameter analyzer (HQ 30D, HACH) to monitor the dissolved O_2 concentration.

SOD-like activity assay

The SOD-like activity of M@Fn-CDs was measured by a SOD detection kit. First, mix 20 μL of the 2 mg mL^{-1} nanozyme solution with 200 μL of the WST-1 working solution containing xanthine. The reaction was then started by adding 20 μL of xanthine oxidase solution. After incubating the reaction solution at 37 °C for 20 minutes, the inhibition rate was calculated by measuring the absorbance at 450 nm using a Molecular Devices M5 Multimode Microplate Reader (USA).

Results and discussion

Synthesis and characterization of metal-doped CDs

Metal-doped CDs (M@Fn-CDs, M = Co, Fe, Cu, Mg, Mn, Ni, Zn, Gd) were fabricated by hydrothermally heating the metal-loaded horse spleen ferritin (M@Fn) for 12 h at 200 °C followed by dialysis for 24 h (Fig. 1a). Metal ions can easily enter the interior of ferritin through the hydrophilic channels in the ferritin shell.[33,34] During the hydrothermal process, metal ions were incorporated into the carbonized protein shells to form M@Fn-CDs. The morphology and size distribution of the as-prepared M@Fn-CDs were characterized by transmission electron microscopy (TEM). As shown in Fig. 1b, the M@Fn-CDs all displayed uniform spherical shapes with sizes ranging from 2 to 4 nm. In contrast, Fn-CDs synthesized using unloaded apoferritin as a precursor appeared as aggregates composed of sub-1 nm carbon clusters, possibly due to structural collapse during carbonization. Near-infrared spectroscopy was used to characterize the functional groups of M@Fn-CDs. FT-IR spectra were obtained after lyophilizing the M@Fn-CDs aqueous solution. As shown in Fig. 1c, the FT-IR spectra of all CDs samples exhibited highly similar features, indicating that they have the same functional groups. These samples exhibited a broad absorption peak at 3000 to 3500 cm^{-1}, corresponding to stretching vibrations of O–H and N–H. The peak around 2955 cm^{-1} was attributed to the asymmetric stretching vibration of the C–H bond. The peak at 1666 cm^{-1} corresponded to the vibration of the C=O/C=N bond. In addition, the peaks at positions 1396 and 1061 cm^{-1} were attributed to C–N and C–O bonds, respectively. From these data, it can be seen that M@Fn-CDs have abundant hydroxyl, carboxyl, and epoxy groups, which impart these materials with excellent water solubility. As shown

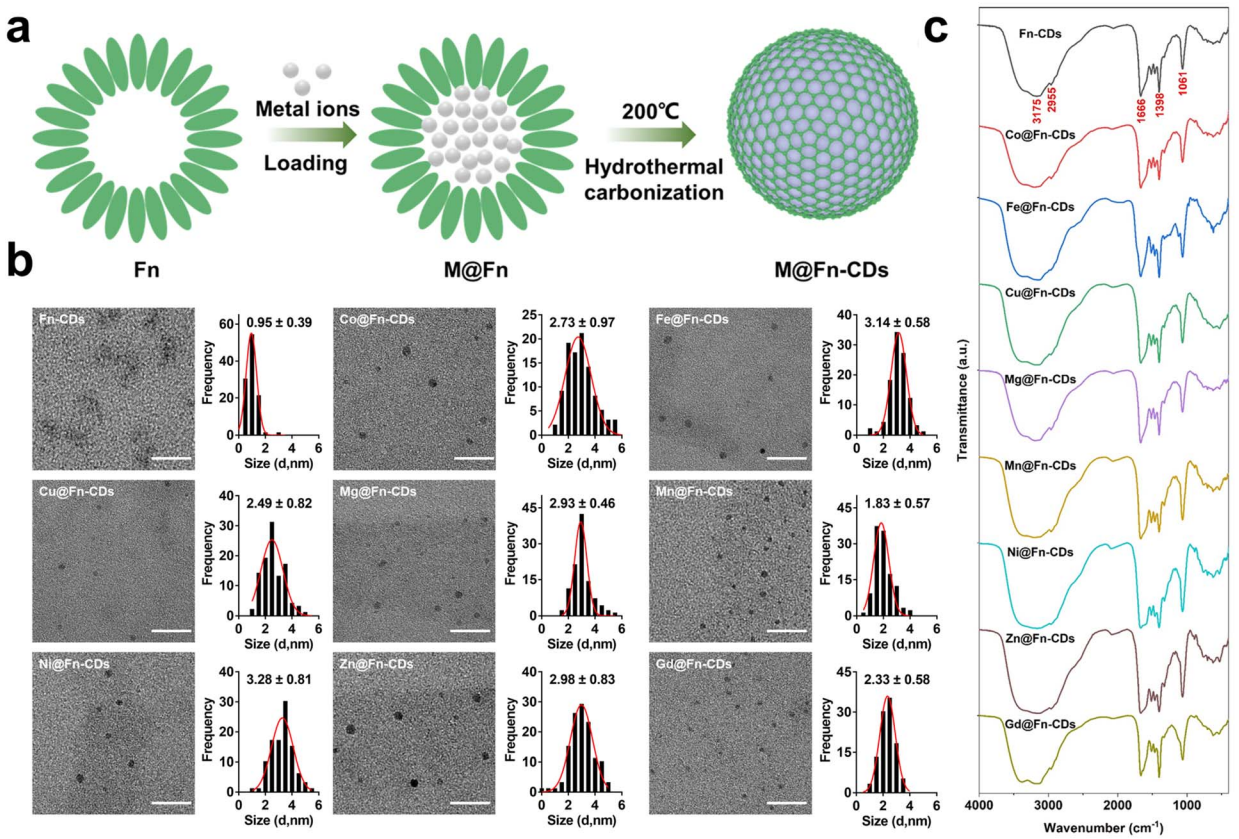

Fig. 1 Synthesis and characterization of Fn-CDs and M@Fn-CDs. (a) Schematic illustration of the synthesis process of M@Fn-CDs. (b) Left: TEM images of M@Fn-CDs. Scale bar = 20 nm. Right: Size histogram of the M@Fn-CDs with curve fitted to the data using a Gaussian model. (c) The FT-IR spectra of M@Fn-CDs.

Table 1 The metal content in M@Fn-CDs determined by ICP-OES

Samples	Metal (wt%)
Co@Fn-CDs	7.44
Fe@Fn-CDs	8.75
Cu@Fn-CDs	6.67
Mg@Fn-CDs	5.72
Mn@Fn-CDs	6.65
Ni@Fn-CDs	2.24
Zn@Fn-CDs	6.76
Gd@Fn-CDs	3.35

in Table 1, the metal content in M@Fn-CDs varied from 2.24% to 8.75%. This difference in metal content may be related to the different efficiency of metal ions entering ferritin. Compared with other metals, Fe ions may be able to enter ferritin more easily, and thus Fe@Fn-CDs had the highest metal content.

Optical properties

The UV-vis absorption, photoluminescence excitation and emission of M@Fn-CDs in aqueous solution were carried out to evaluate their optical properties. The aqueous solutions of M@Fn-CDs all emitted bright yellow fluorescence visible under UV light (Fig. 2a). As shown in Fig. 2b, the UV-vis absorption of M@Fn-CDs exhibited a dominant peak at $\lambda \approx 280$ nm, which was attributed to the aromatic π–π^* transition of the conjugated C=C structure. The fluorescence spectra of Fn-CDs and Fe@Fn-CDs at different excitation wavelengths were shown in Fig. 2c and d, respectively, showing their excitation-dependent fluorescence emission. As the excitation wavelength was gradually increased from 300 to 480 nm (20 nm), a red-shift of the emission peaks of Fn-CDs and Fe@Fn-CDs was observed. The fluorescence intensity gradually decreased as λ_{ex} increased from 320 to 480 nm. Such excitation-tunable emission was considered a universal property of CDs. Under excitation light of 350 nm, the fluorescence emission of all 9 samples was compared. As shown in Fig. 2e, these samples all emitted an emission peak at about 426 nm under excitation at $\lambda_{ex} =$ 350 nm. Then, the integrated fluorescence intensity (emission peak area) as a function of solution absorbance was plotted, and the quantum yields of M@Fn-CDs were calculated with quinine sulfate as a standard reference (Fig. 3). The quantum yields of the nine samples ranged from 5.81% to 10.61%, among which Zn@Fn-CDs exhibited the highest quantum yield. These data demonstrated that metal-doped CDs prepared from ferritin precursors have good optical properties.

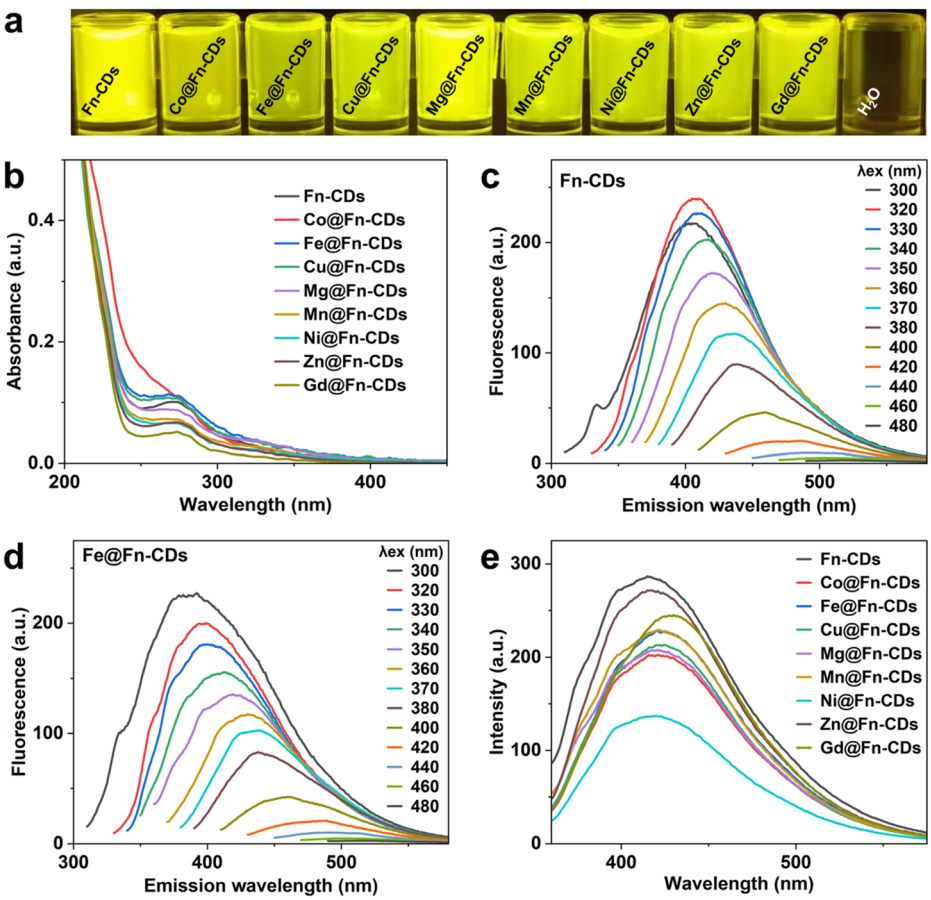

Fig. 2 The optical properties of M@Fn-CDs. (a) Photographs of aqueous solutions of M@Fn-CDs taken under UV light. (b) The UV-vis spectra of M@Fn-CDs. The fluorescence emission spectra of (c) Fn-CDs and (d) Fe@Fn-CDs at different excitation wavelengths from 300 to 480 nm. (e) The fluorescence emission spectra of M@Fn-CDs at 350 nm excitation wavelength.

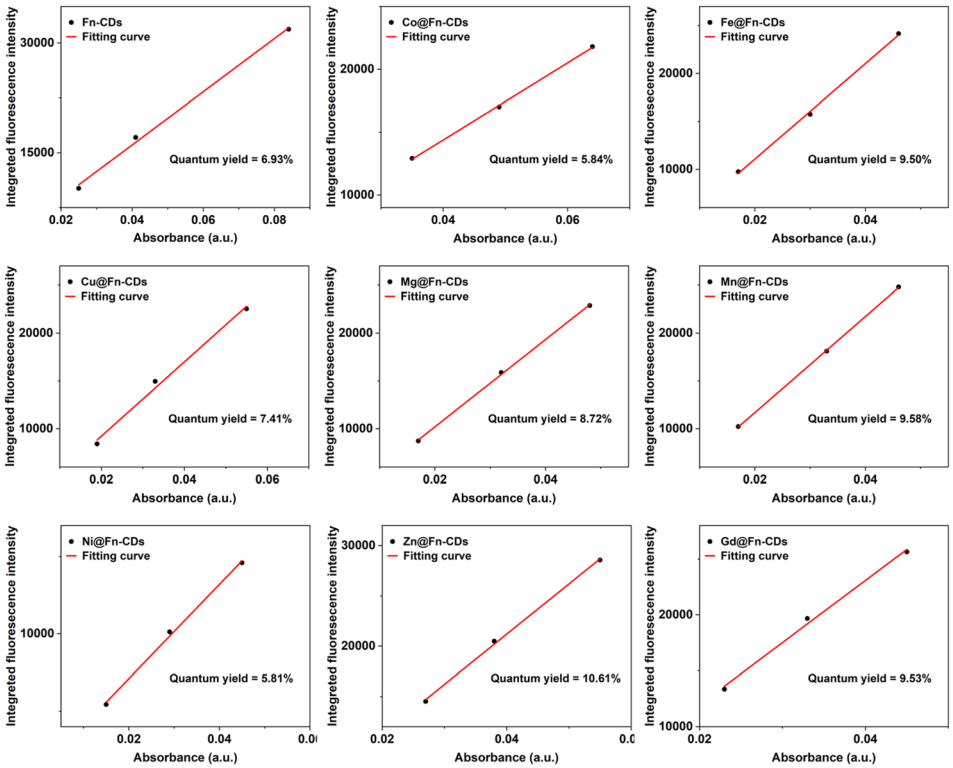

Fig. 3 Quantum yield calculation of M@Fn-CDs. Quantum yields were determined using a slope method, using quinine sulfate as a reference.

Enzyme-like activities

CDs have been reported to be a class of nanozymes with good biocompatibility and multiple enzyme-like catalytic activities. We therefore explored the enzymatic catalytic properties of M@Fn-CDs, including peroxidase, oxidase, catalase, and SOD. The peroxidase-like assay was performed in the TMB–H_2O_2 system, which is a characteristic reaction catalyzed by horseradish peroxidase (HRP). In the presence of H_2O_2, the peroxidase-like nanozyme catalyzes the oxidation of TMB, and the oxidation product exhibits a detectable specific absorbance at 652 nm. As shown in Fig. 4a, M@Fn-CDs exhibited differential peroxidase-like activities, among which Fe@Fn-CDs exhibited the most prominent activity. Metal-free Fn-CDs also exhibited some peroxidase-like activity, which was roughly half that of Fe@Fn-CDs. The peroxidase-like activities of other samples were much lower than those of Fe@Fn-CDs, among which Zn@Fn-CDs and Gd@Fn-CDs hardly showed peroxidase-like activities. The oxidase-like activity was also analyzed using TMB as a substrate in the absence of H_2O_2 (Fig. 4b). Fe@Fn-CDs also showed the best oxidase-like activity among the samples, which was consistent with some reported results.[35] The catalase-like activity of M@Fn-CDs was evaluated by measuring the dissolved oxygen in neutral H_2O_2 solution. The results showed that the amount of dissolved oxygen in the H_2O_2 solution containing Fe@Fn-CDs was significantly increased, indicating that Fe@Fn-CDs possessed catalase-like activity (Fig. 4c). In contrast, the catalase-like activities of other M@Fn-CDs were significantly lower than those of Fe@Fn-CDs. The better catalytic activity of Fe@Fn-CDs than other M@Fn-CDs may be attributed to two reasons. On the one hand, the metal content of Fe@Fn-CDs was higher than that of other M@Fn-CDs, which made it expose more metal sites to participate in the catalysis. On the other hand, proper metal-carbon coordination and catalytic microenvironments that are more favorable for electron transfer may be formed in the structure of Fe@Fn-CDs, which plays an important role in redox catalysis. For instance, single-atom nanozymes with FeN_5 coordination have been reported to exhibit better oxidase-like activity than single-atom nanozymes with other metal coordination.[36] SOD disproportionates superoxide into H_2O_2 and O_2. In our SOD assay system, superoxide produced by the reaction of xanthine with xanthine oxidase (XOD) reduces WST-1 to colorimetrically detectable formazan absorbing at 440 nm. Therefore, the inhibition rate of superoxide anion by M@Fn-CDs can be calculated by measuring the amount of formazan generated. Interestingly, these M@Fn-CDs generally exhibited SOD-like catalytic activity, among which Fe@Fn-CDs and Mg@Fn-CDs were the most prominent. Therefore, we speculated that the SOD-like activity of M@Fn-CDs may mainly originate from its carbon components and surface groups, such as carboxyl groups, which have been reported to play important roles in the SOD-like catalysis of fullerenes.[37] These data suggested that ferritin-derived CDs have intrinsic oxidoreductase-like properties. In particular, Fe@Fn-CDs exhibited significantly enhanced enzymatic activities.

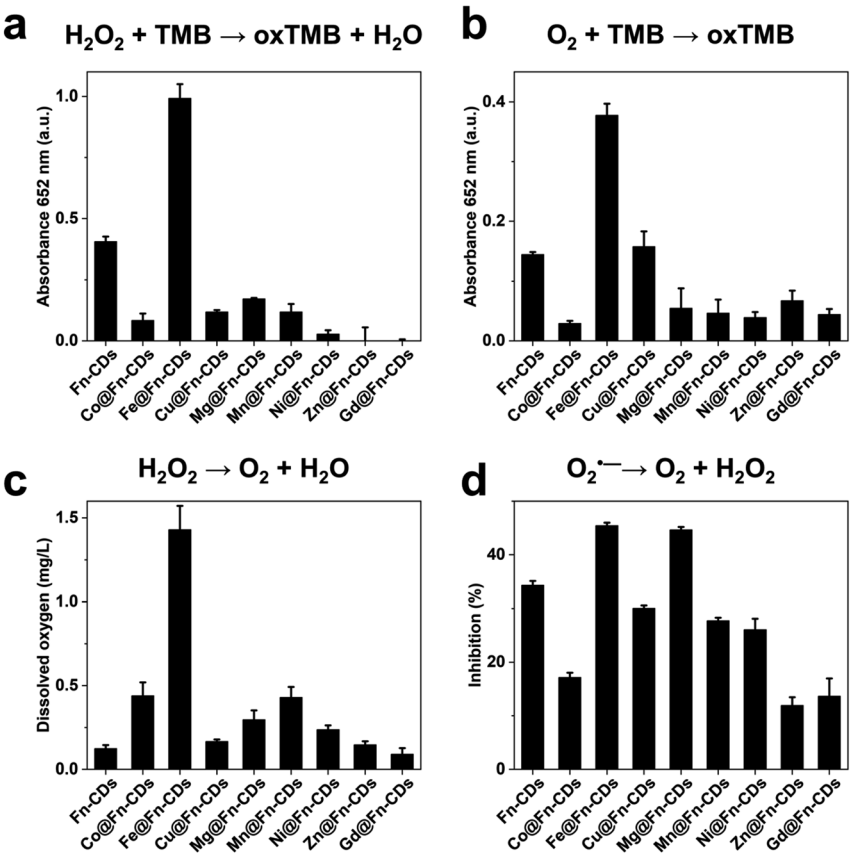

Fig. 4 The enzyme-like activities of M@Fn-CDs. (a) The peroxidase-like activity of M@Fn-CDs measured in the TMB–H_2O_2 system. (b) The oxidase-like activity of M@Fn-CDs measured with TMB as substrate. (c) The catalase-like activity determined by measuring dissolved oxygen in H_2O_2 solution containing M@Fn-CDs. (d) Inhibition of superoxide anion by M@Fn-CDs as determined by a WST-1-based SOD kit.

Conclusions

Utilizing precursors with well-defined metal–organic architectures to synthesize CDs is important for precise control of metal doping. In this study, we explored the feasibility of using metal-loaded ferritin as a precursor to synthesize CDs, which has a well-defined protein shell-metal core structure. The synthesized M@Fn-CDs exhibited uniformly dispersed size, good water solubility, and excellent optical properties. The enzyme-like activities of M@Fn-CDs were measured, in which Fe@Fn-CDs exhibited prominent peroxidase-like, oxidase-like, catalase-like and SOD-like catalytic activities. The one-pot synthesis of ferritin-derived metal-doped CDs developed in this study will provide a new strategy for developing CDs nanozymes with excellent physicochemical properties and enzymatic activity.

Author contributions

Yanfang Shen: conceptualization, methodology, writing-original graft, Ruofei Zhang: investigation, data curation, resources, Ying Wang: supervision, project administration, formal analysis.

Conflicts of interest

There are no conflicts to declare.

Acknowledgements

Authors are grateful to Key Project of Guangdong Province (2018B030335001) for financial support.

References

1 L. Gao, J. Zhuang, L. Nie, J. Zhang, Y. Zhang, N. Gu, T. Wang, J. Feng, D. Yang and S. Perrett, Intrinsic peroxidase-like activity of ferromagnetic nanoparticles, *Nat. Nanotechnol.*, 2007, **2**(9), 577.
2 H. Wei and E. Wang, Nanomaterials with enzyme-like characteristics (nanozymes): next-generation artificial enzymes, *Chem. Soc. Rev.*, 2013, **42**(14), 6060–6093.
3 J. Wu, X. Wang, Q. Wang, Z. Lou, S. Li, Y. Zhu, L. Qin and H. Wei, Nanomaterials with enzyme-like characteristics (nanozymes): next-generation artificial enzymes (II), *Chem. Soc. Rev.*, 2019, **48**(4), 1004–1076.

4 H. Wei, L. Gao, K. Fan, J. Liu, J. He, X. Qu, S. Dong, E. Wang and X. Yan, Nanozymes: a clear definition with fuzzy edges, *Nano Today*, 2021, **40**(10), 101269.
5 R. Zhang, K. Fan and X. Yan, Nanozymes: created by learning from nature, *Sci. China: Life Sci.*, 2020, **63**(8), 1183–1200.
6 Y. Huang, J. Ren and X. Qu, Nanozymes: classification, catalytic mechanisms, activity regulation, and applications, *Chem. Rev.*, 2019, **119**(6), 4357–4412.
7 Z. Wang, R. Zhang, X. Yan and K. Fan, Structure and activity of nanozymes: inspirations for de novo design of nanozymes, *Mater. Today*, 2020, **41**, 81–119.
8 D. Jiang, D. Ni, Z. T. Rosenkrans, P. Huang, X. Yan and W. Cai, Nanozyme: new horizons for responsive biomedical applications, *Chem. Soc. Rev.*, 2019, **48**(14), 3683–3704.
9 R. Zhang, X. Yan and K. Fan, Nanozymes inspired by natural enzymes, *Acc. Mater. Res.*, 2021, **2**(7), 534–547.
10 Q. Wang, H. Wei, Z. Zhang, E. Wang and S. Dong, Nanozyme: an emerging alternative to natural enzyme for biosensing and immunoassay, *TrAC, Trends Anal. Chem.*, 2018, **105**, 218–224.
11 G. Tang, J. He, J. Liu, X. Yan and K. Fan, in *Nanozyme for tumor therapy: surface modification matters*, Exploration, Wiley Online Library, 2021, pp 75–89.
12 A. B. Sengul and E. Asmatulu, Toxicity of metal and metal oxide nanoparticles: a review, *Environ. Chem. Lett.*, 2020, **18**(5), 1659–1683.
13 D. O. Lopez-Cantu, R. B. González-González, E. M. Melchor-Martínez, S. A. H. Martínez, R. G. Araújo, L. Parra-Arroyo, J. E. Sosa-Hernández, R. Parra-Saldívar and H. M. Iqbal, Enzyme-mimicking capacities of carbon-dots nanozymes: properties, catalytic mechanism, and applications–review, *Int. J. Biol. Macromol.*, 2022, **194**, 676–687.
14 Y. Lv, M. Ma, Y. Huang and Y. Xia, Carbon dot nanozymes: How to be close to natural enzymes, *Chem.–Eur. J.*, 2019, **25**(4), 954–960.
15 R. Bandi, M. Alle, C.-W. Park, S.-Y. Han, G.-J. Kwon, N.-H. Kim, J.-C. Kim and S.-H. Lee, Cellulose nanofibrils/carbon dots composite nanopapers for the smartphone-based colorimetric detection of hydrogen peroxide and glucose, *Sens. Actuators, B*, 2021, **330**, 129330.
16 X. Wang, Y. Lu, K. Hua, D. Yang and Y. Yang, Iodine-doped carbon dots with inherent peroxidase catalytic activity for photocatalytic antibacterial and wound disinfection, *Anal. Bioanal. Chem.*, 2021, **413**(5), 1373–1382.
17 Z. Li, W. Liu, P. Ni, C. Zhang, B. Wang, G. Duan, C. Chen, Y. Jiang and Y. Lu, Carbon dots confined in N-doped carbon as peroxidase-like nanozyme for detection of gastric cancer relevant D-amino acids, *Chem. Eng. J.*, 2022, **428**, 131396.
18 L. Su, S. Qin, Y. Cai, L. Wang, W. Dong, G. Mao, S. Feng, Z. Xie and H. Zhang, Co, N-doped carbon dot nanozymes with acid pH-independence and substrate selectivity for biosensing and bioimaging, *Sens. Actuators, B*, 2022, **353**, 131150.
19 M. L. Liu, B. B. Chen, C. M. Li and C. Z. Huang, Carbon dots: synthesis, formation mechanism, fluorescence origin and sensing applications, *Green Chem.*, 2019, **21**(3), 449–471.
20 S. Das, L. Ngashangva, H. Mog, S. Gogoi and P. Goswami, An insight into the mechanism of peroxidase-like activity of carbon dots, *Opt. Mater.*, 2021, **115**, 111017.
21 L. Nilewski, K. Mendoza, A. S. Jalilov, V. Berka, G. Wu, W. K. A. Sikkema, A. Metzger, R. Ye, R. Zhang, D. X. Luong, T. Wang, E. McHugh, P. J. Derry, E. L. Samuel, T. A. Kent, A.-L. Tsai and J. M. Tour, Highly Oxidized Graphene Quantum Dots from Coal as Efficient Antioxidants, *ACS Appl. Mater. Interfaces*, 2019, **11**(18), 16815–16821.
22 J. Zhou, H. Zhou, J. Tang, S. Deng, F. Yan, W. Li and M. Qu, Carbon dots doped with heteroatoms for fluorescent bioimaging: a review, *Microchim. Acta*, 2017, **184**(2), 343–368.
23 X. Li, Y. Fu, S. Zhao, J. Xiao, M. Lan, B. Wang, K. Zhang, X. Song and L. Zeng, Metal ions-doped carbon dots: Synthesis, properties, and applications, *Chem. Eng. J.*, 2022, **430**, 133101.
24 Y. Liu, B. Xu, M. Lu, S. Li, J. Guo, F. Chen, X. Xiong, Z. Yin, H. Liu and D. Zhou, Ultrasmall Fe-doped carbon dots nanozymes for photoenhanced antibacterial therapy and wound healing, *Bioact. Mater.*, 2022, **12**, 246–256.
25 N. Zhao, J. Song and L. Zhao, Metallic Deep Eutectic Solvents-Assisted Synthesis of Cu, Cl-doped Carbon Dots as Oxidase-like and Peroxidase-like Nanozyme for Colorimetric Assay of Hydroquinone and H_2O_2, *Colloids Surf., A*, 2022, 129390.
26 M. Wang, H. Zhu, B. Liu, P. Hu, J. Pan and X. Niu, Bifunctional Mn-Doped N-Rich Carbon Dots with Tunable Photoluminescence and Oxidase-Mimetic Activity Enabling Bimodal Ratiometric Colorimetric/Fluorometric Detection of Nitrite, *ACS Appl. Mater. Interfaces*, 2022, **14**(39), 44762–44771.
27 T. Pan, H. Chen, X. Gao, Z. Wu, Y. Ye and Y. Shen, Engineering efficient artificial nanozyme based on chitosan grafted Fe-doped-carbon dots for bacteria biofilm eradication, *J. Hazard. Mater.*, 2022, **435**, 128996.
28 S. A. Shaik, S. Sengupta, R. S. Varma, M. B. Gawande and A. Goswami, Syntheses of N-doped carbon quantum dots (NCQDs) from bioderived precursors: a timely update, *ACS Sustainable Chem. Eng.*, 2020, **9**(1), 3–49.
29 M. Kumari, G. R. Chaudhary, S. Chaudhary, A. Umar, S. Akbar and S. Baskoutas, Bio-Derived Fluorescent Carbon Dots: Synthesis, Properties and Applications, *Molecules*, 2022, **27**(16), 5329.
30 S. Marouzi, M. Darroudi, A. Hekmat, K. Sadri and R. Kazemi Oskuee, One-pot hydrothermal synthesis of carbon quantum dots from *Salvia hispanica* L. seeds and investigation of their biodistribution, and cytotoxicity effects, *J. Environ. Chem. Eng.*, 2021, **9**(4), 105461.
31 G. n. Jutz, P. van Rijn, B. Santos Miranda and A. Böker, Ferritin: a versatile building block for bionanotechnology, *Chem. Rev.*, 2015, **115**(4), 1653–1701.
32 B. Jiang, L. Fang, K. Wu, X. Yan and K. Fan, Ferritins as natural and artificial nanozymes for theranostics, *Theranostics*, 2020, **10**(2), 687.

33 N. D. Chasteen and P. M. Harrison, Mineralization in ferritin: an efficient means of iron storage, *J. Struct. Biol.*, 1999, **126**(3), 182–194.
34 R. Laghaei, D. G. Evans and R. D. Coalson, Metal binding sites of human H-chain ferritin and iron transport mechanism to the ferroxidase sites: a molecular dynamics simulation study, *Proteins: Struct., Funct., Bioinf.*, 2013, **81**(6), 1042–1050.
35 X. Li, S. Ding, Z. Lyu, P. Tieu, M. Wang, Z. Feng, X. Pan, Y. Zhou, X. Niu and D. Du, Single-Atomic Iron Doped Carbon Dots with Both Photoluminescence and Oxidase-Like Activity, *Small*, 2022, **18**(37), 2203001.
36 L. Huang, J. Chen, L. Gan, J. Wang and S. Dong, Single-atom nanozymes, *Sci. Adv.*, 2019, **5**(5), eaav5490.
37 S. S. Ali, J. I. Hardt, K. L. Quick, J. S. Kim-Han, B. F. Erlanger, T.-t. Huang, C. J. Epstein and L. L. Dugan, A biologically effective fullerene (C60) derivative with superoxide dismutase mimetic properties, *Free Radicals Biol. Med.*, 2004, **37**(8), 1191–1202.